Modelling human brain-wide pigmentation in rodents recapitulates age-related multisystem neurodegenerative deficits

Ariadna Laguna[1,2,3†], Núria Peñuelas[1,2†], Marta Gonzalez-Sepulveda[1,2], Alba Nicolau[1,2], Sébastien Arthaud[4], Camille Guillard-Sirieix[1,2], Marina Lorente-Picón[1,2], Joan Compte[1,2], Lluís Miquel-Rio[5], Helena Xicoy[1], Jiong Liu[4], Annabelle Parent[1,2], Thais Cuadros[1,2], Jordi Romero-Giménez[1], Gemma Pujol[1], Lydia Giménez-Llort[3], Patrice Fort[4], Analia Bortolozzi[5], Iria Carballo-Carbajal[1] & Miquel Vila[1,2,3,6,7]*

[1]Neurodegenerative Diseases Research Group, Vall d'Hebron Research Institute (VHIR)-Network Center for Biomedical Research in Neurodegenerative Diseases (CIBERNED); 08035 Barcelona, Spain

[2]Aligning Science Across Parkinson's (ASAP) Collaborative Research Network; Chevy Chase, MD 20815, USA

[3]Institut de Neurociències-Autonomous University of Barcelona (INc-UAB); 08193 Cerdanyola del Vallès, Spain

[4]Université Claude Bernard Lyon 1, CNRS, INSERM, Centre de Recherche en Neurosciences de Lyon CRNL U1028 UMR5292, SLEEP, 69500 Bron, France

[5]Department of Neuroscience and Experimental Therapeutics, IIBB–CSIC, August Pi i Sunyer Biomedical Research Institute (IDIBAPS)-Center for Networked Biomedical Research on Mental Health (CIBERSAM); 08036 Barcelona, Spain

[6]Department of Biochemistry and Molecular Biology, Autonomous University of Barcelona; 08193 Barcelona, Spain

[7]Catalan Institution for Research and Advanced Studies (ICREA); 08010 Barcelona, Spain

†These authors contributed equally to this work

*Correspondence: miquel.vila@vhir.org

SUMMARY

One key limitation in developing effective treatments for neurodegenerative diseases is the lack of models that accurately mimic the complex physiopathology of the human disease. Humans accumulate with age the pigment neuromelanin inside catecholaminergic neurons. Neurons reaching the highest neuromelanin levels preferentially degenerate in Parkinson's, Alzheimer's and apparently healthy aging individuals. However, this brain pigment is not taken into consideration in current animal models because, in contrast to humans, common laboratory species such as rodents do not produce neuromelanin. Here we generated a tissue-specific transgenic mouse that mimics the human age-dependent brain-wide distribution of neuromelanin within catecholaminergic regions, based on the constitutive catecholamine-specific expression of human melanin-producing enzyme tyrosinase. In parallel to progressive human-like neuromelanin pigmentation, these animals display age-related neuronal dysfunction and degeneration affecting numerous brain circuits and body tissues, linked to motor and non-motor deficits, reminiscent of early neurodegenerative stages. This model may open new research avenues in the field of brain aging and neurodegeneration.

Keywords: neuromelanin, aging, neurodegeneration, Parkinson, substantia nigra, locus coeruleus, dorsal vagal complex, autonomic dysfunction, neuroinflammation.

INTRODUCTION

Humans progressively accumulate with age the dark-brown pigment neuromelanin (NM) within catecholaminergic brain nuclei. NM is formed as a byproduct of catecholamine synthesis and metabolism, beginning with the conversion of tyrosine to L-DOPA, which is then synthesized further to form the neurotransmitters dopamine and noradrenaline, the cytosolic excess of which, if not encapsulated into synaptic vesicles, is oxidized into NM (Sulzer et al., 2000). In contrast to the widespread distribution of other brain pigments such as lipofuscin, NM is thus restricted to catecholamine-producing regions and forms only in neurons. Because neurons do not have the capacity to degrade or eliminate this pigment, NM progressively accumulates with age until occupying most of the neuronal cytoplasm (Halliday et al., 2006). It has long been established that neurons with the highest NM levels, including midbrain dopaminergic neurons from the substantia nigra pars compacta (SNpc/A9) and ventral tegmental area (VTA/A10) and pontine noradrenergic neurons from the locus coeruleus (LC/A6), preferentially degenerate in Parkinson's disease (PD) leading to characteristic motor and non-motor symptoms (Sulzer and Surmeier, 2013). In addition, the LC also degenerates extensively in patients with Alzheimer's disease (AD) (Tomlinson et al., 1981). In both disorders, the LC is in fact one of the first nuclei to become affected, underlying prodromal symptoms such as sleep disorders, anxiety or depression (Braak et al., 2011; Del Tredici and Braak, 2013; Zarow et al., 2003). Even in the absence of overt PD or AD, NM-filled neurons from apparently healthy aged individuals also exhibit early signs of neuronal dysfunction and degeneration compared to young adult brains, including age-related loss of pigmented SNpc and LC neurons, downregulation of phenotypic neuronal markers, alpha-synuclein and tau pathology or the presence of extracellular NM (eNM) released from dying neurons associated with sustained microglial activation (Beach et al., 2007; Chu and Kordower, 2007; Kordower et al., 2013; Mann and Yates, 1979; Xing et al., 2018).

While various factors may contribute to the preferential susceptibility of melanized neurons in neurodegenerative disease and brain aging, including their long and diffuse axonal projections, intrinsic pacemaker activity and high metabolic demand (Sulzer and Surmeier, 2013), the presence of conspicuous intracellular pigment deposits has long been suspected as a key vulnerability factor contributing to their early and extensive demise (Hirsch et al., 1988). However, the potential influence of age-dependent NM accumulation on neuronal function and viability has been largely overlooked in experimental animal modeling because, in contrast to humans, common laboratory animal species such as rodents lack this pigment. Although NM is present in some other species as varied as monkeys (Herrero et al., 1993; Marsden, 1961), dolphins (Sacchini et al., 2018) and frogs (Kemali and Gioffre, 1985), the highly abundant amount of NM in the brainstem, visible with the naked eye, is unique to humans, as NM accumulation increases progressively as the evolutionary relation to man becomes closer (Marsden, 1961). Thus, most of what is known about the formation and potential role of this pigment in both health and disease is inferred from human postmortem analyses (Zucca et al., 2018).

To overcome this major limitation, here we generated a tissue-specific transgenic mouse (termed tgNM) that mimics the progressive, age-dependent brain-wide distribution of pigmentation within all catecholaminergic regions of the human brain. This model is based on the constitutive catecholaminergic-specific expression of the human melanin-producing enzyme tyrosinase (TYR) driven by the tyrosine hydroxylase (TH) promoter. In a previous proof-of-concept study we have shown that unilateral viral vector-mediated expression of TYR restricted to the rodent SNpc induced the production of a NM-like pigment within ipsilateral nigral dopaminergic neurons

virtually analogous to human NM, at levels up to those reached in elderly humans (Carballo-Carbajal et al., 2019). In the latter animals, progressive NM build-up in the SNpc ultimately compromised neuronal function and triggered nigrostriatal degeneration associated to motor deficits (Carballo-Carbajal et al., 2019; Gonzalez-Sepulveda et al., 2023). In the tgNM mice reported here, we found that progressive brain-wide bilateral NM pigmentation is associated to age-related neuronal dysfunction and degeneration affecting numerous brain neurotransmission systems and tissues in the body linked to a myriad of motor and non-motor alterations, equivalent to prodromal/early stages of neurodegeneration.

RESULTS

Brain-wide and age-dependent human-like NM accumulation in tgNM mice

Constitutive and catecholaminergic-specific overexpression of TYR was achieved by classical transgenesis driven by the TH promoter (Tg-TH:TYR mice; tgNM). TYR cDNA expression was assessed in distinct catecholaminergic and non-catecholaminergic dissected brain nuclei from tgNM mice at 12 months (m) of age (Figure S1A). As expected, higher TYR expression was detected within catecholaminergic brain areas compared with non-catecholaminergic regions, with a positive correlation between TYR and TH expression levels (Figure S1A-B). TYR expression was also confirmed at the cellular level by in situ hybridization in tgNM brain tissue sections (Figure S1C). As anticipated from our previous work (Carballo-Carbajal et al., 2019), TYR overexpression resulted in high NM levels in the most PD-vulnerable catecholaminergic regions (SNpc, VTA and LC), appearing as macroscopically visible dark-brown colored areas in the absence of any staining, mimicking their appearance in human specimens (Figure 1A-C and Movie S1). As in humans, melanized SNpc, VTA and LC from tgNM mice could also be detected macroscopically as hyperintense areas by NM-sensitive high-resolution T1-weighted magnetic resonance imaging (Figure 1A-C). Histologically, NM from tgNM mice appeared as a dark-brown neuronal pigment in hematoxylin and eosin-stained sections and stained prominently with the melanin marker Masson-Fontana, similar to melanized human neurons (Figure 1A-C). NM production in tgNM mice was not limited to these major catecholaminergic nuclei but was also present, at varying degrees, in all catecholaminergic cell groups (i.e. A1-A16) (Figure 2A and Table S1), thereby mimicking the pattern of human NM distribution (Saper and Petito, 1982). As in humans (Fedorow et al., 2006), NM is continuously produced throughout life in tgNM mice and progressively accumulates with age until occupying a major portion of the neuronal cytoplasm (Figure S2A-B). In these animals, NM exhibits a caudorostral gradient of accumulation, reaching earlier higher intracellular levels in lower brainstem areas (dorsal vagal complex [DVC] and LC) than in upper brainstem regions (SNpc and VTA) (Figure 2B). These results indicate that TYR expression in tgNM mice leads to the production of human-like NM within all brain catecholaminergic neuronal groups in an age-dependent manner.

Dopaminergic dysfunction and pathology in aged tgNM mice

SNpc and adjacent VTA constitute the main catecholaminergic nuclei in the midbrain and are the primary source of NM in the human brain. Both dopaminergic nuclei degenerate in PD (McRitchie et al., 1997). We assessed the consequences of intracellular NM build-up in terms of viability and function of dopaminergic neurons (Figure S3A). We characterized first the sensorimotor capacities of these animals at different ages (i.e. young [3-4m], adult [8-12m], old [18-20m]), corresponding to progressively increased levels of NM in SNpc and VTA (Figure S2). Adult and old tgNM mice

spent more time to cross a horizontal beam (Figure 3A), indicating impaired motor coordination and balance. Adult and old tgNM mice also exhibited decreased olfactory acuity to discriminate a lemon essence (Figure 3B), indicating impaired olfaction. We also noticed a significant absence of vocalizations during the performance of the behavioral tests that was already present in young tgNM mice (Figure 3C), a phenotype related to cranial sensorimotor deficits previously reported in alpha-synuclein-overexpressing transgenic mice as an early pre-motor manifestation (Grant et al., 2014). Other behavioral tests, such as grip strength and novel object recognition, did not reveal any differences between genotypes at any age (Figure S3B-C). We then performed stereological cell counts of TH-positive neurons in tgNM mice and noted a significant decrease both in SNpc and VTA at adult and old ages (Figure 3D-E). This decrease appeared to correspond to a TH phenotypic downregulation rather than cell loss, as indicated by the presence of dopaminergic NM-containing neurons immunonegative for TH (Figure 3F). These TH-immunonegative pigmented neurons, which are also conspicuously observed in human PD and aged postmortem brains (Korzhevskii et al., 2021; Nagatsu et al., 2019), represent dysfunctional dopaminergic neurons at early stages of degeneration (Carballo-Carbajal et al., 2019; Hirsch et al., 1988). The loss of dopaminergic phenotype was confirmed by decreased transcript expression of dopaminergic markers in SN-VTA dissected tissue from old tgNM mice (Figure S4A). To further assess cell death, we performed stereological cell counts of total NM-containing neurons, including TH-immunopositive and TH-immunonegative neurons, which confirmed a lack of significant cell loss in the SNpc and VTA of tgNM mice (Figure 3G). However, tgNM brain sections showed considerable amounts of extraneuronal NM (eNM) granules, especially at old ages (Figure S4B). The presence of eNM, which derives from dying neurons and is typically observed in PD and aged postmortem brains (Beach et al., 2007; Ishikawa and Takahashi, 1998; Korzhevskii et al., 2021; Langston et al., 1999), indicates an incipient neurodegenerative process in these animals. All these changes were accompanied by reductions of dopaminergic markers in striatal fibers (i.e. TH, dopamine transporter [DAT] and vesicular monoamine transporter 2 [VMAT2]), as measured by Western blot in dissected tissue and/or by optical densitometry in immunostained histological sections (Figure S4C-D). While total dopamine (DA) levels were not changed in tgNM, as analyzed by ultra-performance liquid chromatography (UPLC) in striatal and SN-VTA tissue homogenates (Figure S5A), these animals exhibited alterations in DA metabolic pathways, including decreased DA synthesis and increased catechol oxidation, the latter producing DA oxidized species acting as NM precursors (Gonzalez-Sepulveda et al., 2023) (Figure S5B-C). In addition, striatal DA release, as assessed by in vivo microdialysis, was impaired in adult tgNM mice (Figure S5D), an age concurring with the appearance of behavioral alterations in these animals.

Neuropathologically, NM-containing SNpc and VTA neurons from tgNM mice exhibited intracellular inclusion bodies as typically seen in PD and aged human brains, including cytoplasmic Lewy body (LB)-like inclusions and nuclear Marinesco bodies (MB) (Figure 4A-B). Similar to humans (Kuusisto et al., 2003), both LB and MB were immunopositive for p62, a common component of neuropathological inclusions (Figure 4A-B). More than 60% of p62-positive cytoplasmic inclusions were also immunopositive for alpha-synuclein (Figure 4C). In contrast, as reported in humans (Kuusisto et al., 2003), all MB were immunonegative for alpha-synuclein (Figure 4B). Inclusion body formation was restricted to melanized neurons and was not observed in wt mice. The number of both LB and MB was less prominent in old tgNM, coinciding with the intensification of neurodegenerative changes (i.e. eNM), thus suggesting that inclusion-containing neurons may be those that preferentially start to degenerate (Figure 4A-B). In

agreement with this, the number of neuronal inclusions in PD brains at advanced stages of the disease is much lower than that observed in early PD cases (Braak et al., 2003). Inclusion formation in tgNM mice coincided with decreased expression of autophagy markers (Figure S6A), both reflecting impaired proteostasis in NM-laden brain regions (Carballo-Carbajal et al., 2019). TgNM mice also exhibited early inflammatory changes in the SNpc and VTA, including increased numbers of GFAP-positive astrocytic cells and reactive Iba1-positive microglial cells (Figure 4D and Figure S6B), the latter surrounding eNM as it occurs in postmortem PD brains (Ishikawa and Takahashi, 1998; Langston et al., 1999). Overall, progressive NM production in SNpc and VTA from tgNM mice is associated to age-dependent dopaminergic functional alterations and neuropathological changes linked to incipient neurodegeneration, as similarly observed in aged human brains and prodromal/early PD stages.

Early LC pathology and noradrenergic neurodegeneration in tgNM mice

The LC is a highly melanized region in the pons that constitutes the main source of noradrenaline (NA) modulation in the brain. In addition, the LC is another major area consistently affected in PD, among the earliest sites of Lewy pathology and its degeneration is postulated to precede SNpc involvement and to account for non-motor PD symptoms, including sleep disturbances, anxiety-depression and cognitive decline (Betts et al., 2019; Braak et al., 2003; Knudsen et al., 2018; Zarow et al., 2003). However, the LC is usually neglected in PD research. We next examined the consequences of NM buildup in noradrenergic LC neurons (Figure S7A). First, we assessed the functional integrity of the LC in anxiety-related behavior (open field test), emotional memory (step-down test) and sleep (polysomnography) paradigms. Adult tgNM mice spent more time and travelled more distance in the periphery of an open field than their wt littermates (Figure 5A), despite moving at a similar speed (Figure S7B), indicative of an anxiety-related behavior. Old tgNM animals spent less time on a platform before stepping down and receiving an electric shock, indicative of a deficit in the amygdala-dependent learning and memory process (Figure 5B). Adult tgNM mice exhibited reduced amounts of both paradoxical sleep (PS) and slow-wave sleep (SWS) at the expense of wakefulness (Figure S7C), indicative of an altered sleep-wake cycle. An in-depth analysis of PS evidenced significantly reduced numbers of bouts concomitant to a significant increase of their duration in both adult and old tgNM mice (Figure 5C), indicative of an irreversible dysregulation of PS ultradian rhythm.

Stereological cell counts revealed a marked reduction of TH-positive cells in the LC of tgNM mice compared with wt littermates, which was already present at a pubertal age (1m) (Fig. 5D). In contrast to the SNpc and VTA above, the reduction in TH-positive cells in the LC corresponded to an actual neuronal loss as indicated by stereological cell counts of total noradrenergic NM-containing LC neurons (Figure 5D). We also found abundant eNM at all ages concomitant with cell loss (Figure 5E). LC neurodegeneration resulted in a significant reduction in total NA levels, already evident at a young age, in both LC and its projecting areas such as the prefrontal cortex (Figure 5F). These animals also exhibited reduced NA synthesis and increased NA degradation (Figure S7D), indicating altered NA neurotransmission. Melanized LC neurons also exhibited p62-positive cytoplasmic inclusions but almost no MB were detected (Figure 5G) and Figure S7E). The highest number of LC cytoplasmic inclusions were found at pubertal ages and decreased afterwards (Figure 5G), possibly due to the high degree of neuronal loss in this area with only a few remaining neurons left (Figure 5D). Most of these inclusions were also immunoreactive for alpha-synuclein (Figure S7F). Concomitant to neurodegeneration, the LC from tgNM mice exhibited marked inflammatory changes from a young age, including astrocytosis and microglial

activation (Figure 5H and Figure S7G). Altogether, tgNM mice exhibit an early and extensive degeneration of the LC, linked to non-motor alterations, that precedes nigral dopaminergic dysfunction, similar to prodromal/early PD stages (Betts et al., 2019; Knudsen et al., 2018; Zarow et al., 2003).

Cholinergic and serotonergic alterations in tgNM mice

In addition to catecholaminergic pigmented areas, non-pigmented neurons also degenerate in PD, in particular cholinergic neurons from the nucleus basalis of Meynert (NBM) and the pedunculopontine nucleus (PPN) (Giguere et al., 2018). These two cholinergic nuclei are vastly connected with the brainstem PD-vulnerable catecholaminergic areas (French and Muthusamy, 2018; Gratwicke et al., 2013; Mena-Segovia and Bolam, 2017; Tubert et al., 2019) (Figure S8A), and their degeneration in PD may be related to the degeneration of the interconnected melanized neurons from the SNpc, VTA and LC (Bensaid et al., 2016; Szego et al., 2011). We detected a significant decrease in the total number of choline acetyltransferase (ChAT)-positive neurons in the NBM and PPN nuclei in old tgNM mice (Figure 6A-B and Figure S8B). However, total acetylcholine (Ach) levels were not decreased in the cortex of old tgNM animals, and they were actually increased in the PPN itself (Figure 6C).

Another neurotransmitter system often altered in PD is the serotonergic system. Indeed, anxiety and depression are common non-motor symptoms affecting 30-35% of PD patients (Aarsland et al., 2011; Chuquilin-Arista et al., 2020; Miquel-Rio et al., 2022). Variable degrees of cell death have been reported in the raphe nuclei from PD postmortem brains (Giguere et al., 2018). We assessed the integrity of the dorsal raphe (DR) nucleus in tgNM mice. Stereological cell counts of tryptophan hydroxylase (TPH)-positive serotonergic DR neurons did not show statistically-significant differences in old tgNM mice, although these numbers were overall lower than in wt littermates (Figure 6D). Of note, some TPH-positive DR cells (~3%) contained NM, which is compatible with these neurons being also catecholaminergic, as previously described (McDevitt et al., 2014; Trulson et al., 1985). No significant changes were found in serotonin (5-HT) levels in the DR nor in the PFC of tgNM mice (Figure 6E). Still, tgNM mice exhibited increased immobilization time in the tail suspension test, indicative of a depressive-like behavior (Cryan et al., 2005) (Figure 6F).

NM accumulation in medullary nuclei associated to autonomic dysfunction in tgNM mice

Pigmented catecholaminergic neuronal groups in the caudal medulla have also been reported to degenerate in PD, in particular NM-containing neurons of the dorsal motor nucleus of the vagus region (Gai et al., 1993; Halliday et al., 1990; Rajput and Rozdilsky, 1976; Saper et al., 1991). These neurons, which are part of the dorsomedial medullary A2 group and present both noradrenergic and adrenergic cells, intermingle with cholinergic neurons of the dorsal motor nucleus of the vagus nerve (DNV) and nucleus of the solitary tract (NTS) to constitute an overlapped structure referred to as the DVC, which altogether provide the major integrative center for the mammalian autonomic nervous system. We next characterized the viability of DVC pigmented neurons in tgNM mice (Figure 7A and Figure S9A). Stereological cell counts of TH-positive and total catecholaminergic neurons in DVC sections showed no consistent decreases in tgNM mice compared with wt littermates (Figure S9B). However, only a small percentage (~10%) of TH-positive neurons in the DVC were actually pigmented. Hence, we evaluated only the pigmented TH-positive neurons and found a significant decrease of these cells with age (Figure 7B). In adult tgNM mice, this decrease mostly corresponded to a phenotypic TH-downregulation,

as the number of total pigmented cells was not yet reduced at this stage (Figure 7C). Reduced number of pigmented TH-positive DVC neurons was accompanied by extensive eNM and microglial activation (Figure 7D-E and Figure S9C). A few cytoplasmic inclusions were also detected in melanized DVC neurons, but only at pubertal ages preceding phenotypic loss in adult ages (Figure 7F). In contrast, ChAT-positive DVC cells were not affected in tgNM mice (Figure S9D).

To evaluate the functional consequences of medullary DVC alterations, we assessed autonomic parameters (cardiovascular, respiratory and gastrointestinal) in tgNM mice (Figure 8A). Old tgNM mice showed decreased heart rate (Figure 8B), despite no apparent alterations in blood pressure (Figure 8C). These animals also exhibited increased respiratory rate by measuring diaphragmatic movements (Figure 8D). In contrast, no changes in gastrointestinal function were found in tgNM mice by measuring intestinal transit time with oral red carmine administration (Figure 8K). Concomitant with these signs of peripheral autonomic dysfunction, we detected a significant decrease in DA and NA levels, as well as altered synthesis and degradation, in the DVC of tgNM mice (Figure 8F and Figure S9E). In addition, alterations in NA and Ach levels were also detected in vagal-innervated peripheral organs of tgNM mice like the heart and intestines (Figure 8F). Dysautonomic disorders, in particular cardiovascular and respiratory, are reported to be more frequent causes of death in PD than in age-matched controls[40,41]. We evaluated life expectancy in tgNM mice and detected a decreased lifespan compared to their wt counterparts (median survival of TgNM mice: 20.7m; Figure 8G). Overall, in addition to the brain-related alterations reported above, our results reveal that tgNM mice also recapitulate some of the peripheral autonomic alterations occurring in PD.

DISCUSSION

Modelling the physiopathology of neurodegenerative diseases remains a difficult task. Several animal models have been developed to understand disease pathogenesis and test new drug candidates. However, neurodegenerative diseases are highly heterogeneous diseases involving several factors and pathways. Therefore, none of the existing models replicates the entire spectrum of clinical and neuropathological features occurring in neurodegenerative diseases. Here we provide a new animal model that fills a significant gap in the field by incorporating in rodents a human factor intimately linked to brain aging and neurodegeneration such as NM, which has been so far neglected in experimental preclinical *in vivo* research. Indeed, because NM is not spontaneously produced in the most commonly used laboratory animals, such as rodents, work on this pigment has been so far limited to a small number of studies using scarcely available human brain tissue. Consequently, many aspects of the biology of NM remain to be elucidated. While NM shares some features with melanin found in the periphery (e.g. skin, hair), peripheral melanin is structurally, functionally and compositionally different from NM. Peripheral melanogenesis occurs within specialized cells (i.e. melanocytes) through a biosynthetic pathway enzymatically driven by TYR as the key, rate-limiting enzyme (Slominski et al., 2004). In contrast, the presence of TYR in the human brain, that we and others have reported to be expressed at very low levels (Carballo-Carbajal et al., 2019; Greggio et al., 2005; Miranda et al., 1984; Vila, 2019; Xu et al., 1997), is still disputed (Ikemoto et al., 1998; Plum et al., 2016; Tribl et al., 2007; Tribl et al., 2006; Vila, 2019). In fact, it is widely assumed that NM may be produced by spontaneous nonenzymatic dopamine auto-oxidation (Monzani et al., 2018). However, experimentally increasing dopamine or oxidized dopamine levels in rodents, either with chronic L-dopa treatment (Burbulla et al., 2017;

Murer et al., 1998) or by genetically enhancing TH activity (Mor et al., 2017), is not sufficient by itself to produce NM in these animals, as it might be expected if NM represents a mere process of DA autoxidation. Remarkably, synthetic melanin produced in a test tube by oxidizing dopamine with TYR resembles more closely NM, in terms of absorbance spectra, elemental composition and melanic components, than synthetic melanin obtained by dopamine autoxidation (Cai et al., 2023; Chand et al., 2023). We have previously corroborated, and extended it here, that the neuronal pigment induced by TYR overexpression in rodent catecholaminergic neurons is indeed very similar to human NM, including: (i) its detection by NM-sensitive magnetic resonance imaging, which reflects NM's avid binding of iron (Carballo-Carbajal et al., 2019); (ii) its chemical composition by UPLC-MS/MS, comprising all NM's melanic components (Gonzalez-Sepulveda et al., 2023; Gonzalez-Sepulveda et al., 2020); or (iii) its ultrastructure by electron microscopy, exhibiting an electron-dense matrix associated to characteristic lipid droplets within autophagic compartments (Carballo-Carbajal et al., 2019). This complex structure, including melanic, lipid, peptide and inorganic components contained inside special autolysosomes is a defining hallmark of true NM as opposed to peripheral melanin (Zucca et al., 2023). Therefore, independently of the current debate around the endogenous expression and role of TYR in the human brain, the neuronal pigment produced in tgNM mice can be considered as analogous to human NM, thereby supporting the relevance of our approach to study the impact of human-like NM pigment on age-dependent neuronal function and viability *in vivo*.

The functional significance of NM production, if any, is not currently known. This pigment was long considered just a waste product of catecholamine metabolism devoid of any physiological function. More recently, it has been hypothesized that NM could play a neuroprotective role by removing excessive cytosolic catecholamine oxidized species, chelating potentially toxic metals or sequestering environmental neurotoxins (Zucca et al., 2014). However, a putative protective effect of NM has never been formally demonstrated, probably because of the lack of proper experimental models, and thus remains speculative to this day. In any case, even if we consider NM synthesis to be an initially beneficial process, this is compatible with a deleterious effect of its long-term age-dependent accumulation, by ultimately interfering with normal cell function and proteostasis in addition to an excess production of potentially toxic oxidized catechol intermediates, as we observed in NM-producing rodents (Carballo-Carbajal et al., 2019; Gonzalez-Sepulveda et al., 2023; Vila et al., 2019). Supporting this concept, reduction of intracellular NM accumulation in AAV-TYR-injected rats, either by boosting NM cytosolic clearance with autophagy activator TFEB or by delaying age-dependent NM production through VMAT2-mediated enhancement of dopamine vesicular encapsulation, resulted in a major attenuation of their neurodegenerative phenotype, both at the behavioral and neuropathological level (Carballo-Carbajal et al., 2019; Gonzalez-Sepulveda et al., 2023). In contrast, in absence of associated NM formation, TYR expression was not apparently toxic *per se*, as indicated by a lack of NM production and degeneration of TYR-expressing gamma-aminobutyric acid nigrotectal neurons in AAV-TYR-injected rats (Carballo-Carbajal et al., 2019).

Our results in tgNM mice suggest that age-dependent brain-wide pigmentation, as it occurs in humans, may be sufficient to ultimately trigger a progressive neurodegenerative phenotype with motor and non-motor deficits, affecting multiple neuronal systems in the brain, beyond the SNpc, as well as peripheral organs, all reminiscent of what is observed in prodromal/early PD stages. Brain pigmentation in tgNM mice follows a caudorostral gradient of accumulation that parallels the occurrence of neuropathological alterations observed in PD, reaching higher levels of pigmentation and neuronal pathology earlier in the medulla and pons than in midbrain nuclei

(Halliday et al., 1990; Mann and Yates, 1979; Zecca et al., 2004). In this context, the caudorostral gradient of alpha-synuclein pathology reported in PD brains (Braak et al., 2003) may be linked to a gradient of increasing intracellular NM levels promoting Lewy pathology. In agreement with this, alpha-synuclein has been reported to redistribute to the NM pigment in early stages of PD and become entrapped within NM granules, which may predispose melanized neurons to precipitate alpha-synuclein around pigment-associated lipids under oxidative conditions, such as those linked to NM formation (Fasano et al., 2003; Halliday et al., 2005; Zucca et al., 2018). Our findings also suggest that the neuroinflammatory changes found in human non-diseased aged and PD brains (Beach et al., 2007; Cebrian et al., 2014; Hirsch and Hunot, 2009; Korzhevskii et al., 2021) may actually start prior to overt neurodegeneration and be linked to the presence of incipient eNM released from early degenerating neurons.

Because all humans accumulate NM with age, our results in NM-producing rodents imply that all humans could potentially develop NM-linked neurodegenerative changes if they were to live long enough to reach pathogenic levels of intracellular NM. However, and focusing on PD, only a fraction of the aging population actually develops overt neurodegenerative disease (e.g. up to ~5% of the population over 60 in the case of PD, increasing with age (de Lau and Breteler, 2006)). Yet, in absence of clinically diagnosed PD: (i) 10-30% of apparently healthy people older than 60 years already exhibit Lewy pathology in their melanized brainstem nuclei (i.e. incidental Lewy body disease, who are considered to represent early, presymptomatic stages of PD) (DelleDonne et al., 2008); (ii) parkinsonian signs such as bradykinesia, stooped posture and gait disturbance are common in elderly individuals, reaching a prevalence of up to 50% in individuals over 80 years of age (Bennett et al., 1996; Prettyman, 1998); (iii) multiple reports have documented an age-related loss of pigmented nigral neurons, estimated at about 5-10% per decade, in otherwise healthy individuals (Beach et al., 2007; Mann and Yates, 1979; Xing et al., 2018); (iv) brains from aged individuals commonly exhibit a downregulation of dopaminergic phenotypic markers within melanized nigral neurons, which reflects neuronal dysfunction at early stages of neurodegeneration, as well as abundant eNM released from dying neurons associated with sustained microglial activation, compared to young adult brains (Beach et al., 2007; Chu and Kordower, 2007; Kordower et al., 2013). These observations, combined with our results in NM-producing rodents, suggest that progressive NM accumulation may not be just an innocuous consequence of normal catecholaminergic neuronal aging, as it is currently regarded, but underlie incipient age-dependent functional/degenerative changes in these neurons that would clinically manifest as overt neurodegenerative disease once a certain level of NM accumulation and subsequent cell dysfunction/death is reached. In agreement with this, intracellular NM levels are increased in dopaminergic nigral neurons of PD patients and subjects with incidental Lewy body disease, compared to age-matched healthy individuals, indicating that they may have reached earlier a pathogenic threshold of intracellular NM accumulation (Carballo-Carbajal et al., 2019; Halliday et al., 2005; Vila, 2019). Additional elements, such as genetic or environmental factors, could potentially accelerate or trigger pathology in these already vulnerable NM-filled neurons. Age-dependent brain pigmentation may thus represent a key molecular substrate underlying the well-established association between aging and increased risk of neurodegenerative disease.

Overall, the tgNM mouse model reported here, now readily available to the entire scientific community, provides the opportunity to experimentally address all of these questions in a human-relevant context. These humanized animals recapitulate the biological and temporal complexity of age-dependent neurodegeneration, affecting numerous brain neurotransmission systems and tissues in the body leading to a myriad of motor and non-motor symptoms. Because of the

prodromal nature of these changes, these animals could be combined with additional disease-relevant genetic or environmental manipulations. In addition, these animals could also be used to test potential therapeutic strategies in a human disease state-informed context at different stages of the disease, which should facilitate the translation of findings to humans. The failure, to date, of many rodent model-based findings to translate to clinical utility in the context of age-related neurodegenerative disease strengthens the importance of introducing into *in vivo* research a human factor so intimately linked to brain aging and neurodegeneration such as NM.

ACKNOWLEDGMENTS

We are grateful to: the Neurological Tissue Bank of the Biobanc-Hospital Clinic-IDIBAPS (Barcelona, Spain) and the Biobanco en Red de la Región de Murcia-BIOBANC-MUR (Murcia, Spain) for human sample procurement; Sandra Lope-Piedrafita (UAB, Barcelona, Spain) for technical assistance in the performance of MRI experiments in rodents; the Mesoscopic Imaging Facility (MIF) at the European Molecular Biology Laboratory (EMBL) (Barcelona) for support in brain clarification procedures; Sandra Mancilla from the Unit 20 of CIBER in Bioengineering, Biomaterials & Nanomedicne (CIBER-BBN) at VHIR (Barcelona, Spain) and Beatriz Rodríguez-Galván (VHIR) for assistance in histological processing; Ignasi Sahún from the Phenotyping Unit at Parc Científic de Barcelona (Barcelona, Spain), Guillem Colell and Anna Pujol from the Laboratory Animal Service at VHIR, and Pamela Dominguez at VHIR for assistance in animal behavior; Eliana Markidi for immunoblot analyses and laboratory assistance; Alex Rovira (Neuroradiology section, Vall d'Hebron Hospital, Barcelona, Spain) for providing the human NM-MRI images; Ellen Gelpi (Neurological Tissue Bank, Hospital Clínic-IDIBAPS, Barcelona, Spain & Institute of Neurology, Medical University of Vienna, Austria) for providing the human autopsy images; Dr. Takafumi Hasegawa (Department of Neurology, Tohoku University School of Medicine, Sendai, Japan) for kindly providing the TYR plasmid; Dr. Jin Son and Dr. José López-Barneo from Hospital Virgen del Rocío (Sevilla, Spain) for kindly providing the rat TH promoter plasmid; Prof. Kazumasa Wakamatsu and Prof. Shosuke Ito (Fujita Health University, Aichi, Japan) for kindly donating the 5SCD and 5SCDA standards; Professor Gary Miller (Emory University, USA) for kindly donating the VMAT2 antibody. All diagrams and schematic experimental plans were created with BioRender.com.

AUTHOR CONTRIBUTIONS

Conceptualization, M.V.; Methodology & Formal Analysis, A.L., N.P., M.G-S., A.N., S.A., C.G-S., M.L-P., J.C., Ll.M-R., H.X., J.L., A.P., T.C., J.R-G., Ll-R., G.P., L.G-Ll., P.F., A.Bo., I.C-C., M.V.; Writing-Original Draft, A.L., N.P., M.V.; Writing-Review & Editing, all authors; Supervision, A.L., M.V.

FUNDING

Aligning Science Across Parkinson's through The Michael J. Fox Foundation for Parkinson's Research, USA (ASAP-020505 to MV); The Michael J. Fox Foundation for Parkinson's Research, USA (MJFF-007184 and MJFF-001059 to MV); Ministry of Science and Innovation (MICINN), Spain (PID2019-105136RB-100 to AB and PID2020-116339RB-I00 to MV); EU Joint Programme Neurodegenerative Disease Research (JPND), Instituto de Salud Carlos III, EU/Spain

(AC20/00121 to MV): La Caixa Bank Foundation, Spain (INPhINIT fellowship, code LCF/BQ/DI18/1166063 to JC; Junior Leader Fellowship LCF/BQ/PR19/11700005 to AL; Health Research Grant, ID 100010434 under the agreement LCF/PR/HR17/52150003 to MV) ; Parkinson's U.K. (to MV); Research grants from Association France Parkinson and Fondation Neurodis (to PF); Ministry of Economy and competitiveness (MINECO), Spain with co-funding from FEDER (E.U.) (SAF2015-73997-JIN to AL); Ministry of Economy and competitiveness (MINECO), Spain (BES-2017-080191 to NP).

DECLARATION OF INTERESTS

The Authors declare no competing financial interests.

RESOURCE AVAILABILITY

Lead contact

Further information and requests for resources and reagents should be directed to and will be fulfilled by the Lead Contact, Miquel Vila (miquel.vila@vhir.org).

FIGURE LEGENDS

Figure 1. Accumulation of human-like NM in PD-vulnerable catecholaminergic brain nuclei from TgNM mice. (**A-C**) From *left* to *right*, unstained macroscopic view, NM-sensitive high-resolution T1-weighted magnetic resonance imaging, hematoxilin-eosin (H&E) and Masson-Fontana (M-F) staining of aged healthy human postmortem brains (A), wt (B) and tgNM (C) mice. In C (*right panel*), macroscopic view of a clarified tgNM brain. Unstained NM, brown (see also Movie S1). Scale bars: 20 µm (H&E), 5 µm (M-F). Macroscopic human midbrain image adapted from (Carballo-Carbajal et al., 2019).

Figure 2. Brain-wide NM distribution and accumulation of human-like NM in PD-vulnerable catecholaminergic brain nuclei from TgNM mice. (**A**) Qualitative mouse brain atlas showing NM accumulation in all catecholaminergic groups in tgNM mice (see also Supplementary Table 1). *Left*, Mouse brain atlas. Number of dots represents the quantity of NM-accumulating cells and dot color represents the levels of intracellular NM from very low levels (blue) to higher levels (red). Image credit: Allen Institute. *Right*, chatecholaminergic areas immunostained for TH in wt mice and Nissl-stained in tgNM mice. Unstained NM, brown. Scale bars: 25 µm, 25µm (inset). (**B**) Quantification of intracellular NM levels in unstained SN/A9, VTA/A10, LC/A6, and DVC/A2 brain sections from tgNM mice *$p \leq 0.05$ compared with A9, #$p \leq 0.05$ compared with A10, \$$p \leq 0.05$ compared with A2. Box plots: median, min-max values and individual dots for each neuron. Genotypes, ages, sample sizes and statistical analyses (Data S1).

Figure 3. Dopaminergic dysfunction in tgNM mice. (**A**) Time to cross the beam in seconds (s). (**B**) Olfactory discrimination index. (**C**) Percentage of animals vocalizing. (**D**) SNpc and VTA immunostained sections. TH, blue; unstained NM, brown. Scale bars: 500 µm, 20µm (inset). (**E**) Cell counts of SNpc and VTA TH-positive neurons. (**F**) *Left*, quantification of TH downregulation measured as the percentage (%) of TH-immunonegative neurons within the total population of NM-containing neurons in tgNM mice. *Right*, TH-immunostained SNpc showing $TH^{-}NM^{+}$ (arrow)

and TH^+NM^+ (arrowhead) neurons. (**G**) Cell counts of total SNpc and VTA dopaminergic neurons. In A-C, E-F; *p≤0.05 compared with wt littermates. Box plots: median, min-max values and individual dots for each animal. Genotypes, ages, sample sizes and statistical analyses (Data S1).

Figure 4. PD-like neuropathology in tgNM mice. (**A-B**) *Left*, SNpc and VTA sections exhibiting NM-laden neurons with cytoplasmic (A) and nuclear (B) inclusions. TH, purple; p62, green; alpha-synuclein (Syn), red; Hoechst (blue); NM, dark grey. Scale bar: 10 µm. *Right*, quantification of SNpc and VTA NM-laden neurons with p62-positive cytoplasmic (A) and nuclear (B) inclusions. (**C**) Percentage of SN-VTA cytoplasmic inclusions positive or negative for Syn in tgNM at different ages. (**D**) *Left*, reactive (top) and non-reactive (middle) Iba1-positive microglia (blue) and GFAP-positive astrocytes (bottom, blue). Scale bar: 20 µm. *Right*, quantification of reactive Iba1- and GFAP-positive cells in SNpc and VTA sections. In B; *p≤0.05 compared with young tgNM. In D; *p≤0.05 compared with wt littermates. Box plots: median, min-max values and individual dots for each animal. Genotypes, ages, sample sizes and statistical analyses (Data S1).

Figure 5. Noradrenergic neurodegeneration and PD-like neuropathology in tgNM mice. (**A**) Percentage of time spent and distance travelled in the periphery compared with the center of an open field. **(B**) Time spent on the platform of a step-down test. (**C**) Number and mean duration (s, seconds) of paradoxical sleep (PS) bouts. (**D**) *Left*, LC sections immunostained for TH. TH, blue; unstained NM, brown. Scale bars: 200 µm, 20µm (inset). *Right*, cell counts of LC TH-positive neurons and total NA neurons at different ages. (**E**) Number of eNM granules in tgNM mice. (**F**) LC and prefrontal cortex (PFC) NA levels in young/old tgNM and wt mice. (**G**) *Left*, LC section exhibiting a NM-laden neuron with a cytoplasmic inclusion. TH, purple; p62, green; alpha-synuclein (Syn), red; Hoechst (blue); NM, dark grey. Scale bar: 5 µm. *Right*, quantification of LC NM-laden neurons with p62-positive cytoplasmic inclusions in tgNM mice. (**H**) Images and quantification of reactive Iba1- and GFAP-positive cells in LC sections. In A-D, F, H; *p≤0.05 compared with wt littermates. Box plots: median, min-max values and individual dots for each animal. Genotypes, ages, sample sizes and statistical analyses (Data S1).

Figure 6. Cholinergic and serotonergic alterations in tgNM mice. (**A-B**) *Left*, NBM and PPN sections immunostained for choline acetyltransferase (ChAT). ChAT, blue; unstained NM, brown. Scale bars: 500 µm, 20 µm (inset). *Right*, cell counts of NBM and PPN ChAT-positive neurons in old tgNM and wt mice. (**C**) PPN and prefrontal cortex (PFC) acetylcholine (Ach) levels. (**D**) *Left*, dorsal raphe (DR) sections immunostained for tryptophan hydroxylase (TPH). TPH, blue; unstained NM, brown. Scale bars: 200 µm, 20 µm (inset). *Right*, Cell counts of DR TPH-positive neurons in old tgNM and wt mice. (**E**) DR and PFC serotonin (5HT) levels. (**F**) Immobilization time in the tail suspension test (s, seconds). In A-C, F; *p≤0.05 compared with wt littermates. Box plots: median, min-max values and individual dots for each animal. Genotypes, ages, sample sizes and statistical analyses (Data S1).

Figure 7. Medullary catecholaminergic nuclei alterations in tgNM mice. (**A**) Medullary sections immunostained for TH and ChAT. TH, red; ChAT, blue; unstained NM, brown. Scale bars: 200µm, 10µm (insets). Dorsal motor nucleus of the vagus nerve, DNV; dorsal vagal complex, DVC. (**B-C**) Cell counts of TH-positive (B) and total (C) pigmented catecholaminergic cells. (**D**) *Left*, image of eNM granules (white arrowhead). Scale bar: 25 µm. *Right*, number of eNM granules in A2 neuronal group in tgNM mice. (**E**) Images and quantification of Iba1-positive reactive microglia in tgNM and wt mice. **(F**) *Top*, DVC section exhibiting a NM-laden neuron with a cytoplasmic inclusion. TH, purple; p62, green; alpha-synuclein (Syn), red; Hoechst (blue); NM, dark grey. Scale bar: 5 µm. *Bottom*, quantification of DVC NM-laden neurons with p62-positive

cytoplasmic inclusions in tgNM mice. In B-D; *$p \leq 0.05$ compared with young tgNM. In E; *$p \leq 0.05$ compared with wt littermates. In F; $p \leq 0.05$ compared with adult and old tgNM. Box plots: median, min-max values and individual dots for each animal. Genotypes, ages, sample sizes and statistical analyses (Data S1).

Figure 8. Autonomic dysfunction and decreased lifespan in tgNM mice. (**A**) Schematic diagram of the peripheral A2 innervation sites. (**B**) Heart rate (bpm, beats per minute) in tgNM and wt mice. (**C**) Systolic and diastolic blood pressure in old tgNM and wt mice. (**D**) Respiratory rate (number of breaths/min) in old tgNM and wt mice. (**E**) Intestinal transit time (min, minutes) in old tgNM and wt mice. (**F**) Levels of DA, NA and Ach in DVC and peripheral organs from tgNM and wt mice. (**G**) Survival analysis of tgNM mice compared with wt. m, months. In B-G; *$p \leq 0.05$ compared with wt littermates. Box plots: median, min-max values and individual dots for each animal. Genotypes, ages, sample sizes and statistical analyses (Data S1).

REFERENCES

Aarsland, D., Pahlhagen, S., Ballard, C.G., Ehrt, U., and Svenningsson, P. (2011). Depression in Parkinson disease--epidemiology, mechanisms and management. Nature reviews Neurology *8*, 35-47.

Beach, T.G., Sue, L.I., Walker, D.G., Lue, L.F., Connor, D.J., Caviness, J.N., Sabbagh, M.N., and Adler, C.H. (2007). Marked microglial reaction in normal aging human substantia nigra: correlation with extraneuronal neuromelanin pigment deposits. Acta Neuropathol *114*, 419-424.

Bennett, D.A., Beckett, L.A., Murray, A.M., Shannon, K.M., Goetz, C.G., Pilgrim, D.M., and Evans, D.A. (1996). Prevalence of parkinsonian signs and associated mortality in a community population of older people. NEnglJMed *334*, 71-76.

Bensaid, M., Michel, P.P., Clark, S.D., Hirsch, E.C., and Francois, C. (2016). Role of pedunculopontine cholinergic neurons in the vulnerability of nigral dopaminergic neurons in Parkinson's disease. ExpNeurol *275 Pt 1*, 209-219.

Betts, M.J., Kirilina, E., Otaduy, M.C.G., Ivanov, D., Acosta-Cabronero, J., Callaghan, M.F., Lambert, C., Cardenas-Blanco, A., Pine, K., Passamonti, L., *et al.* (2019). Locus coeruleus imaging as a biomarker for noradrenergic dysfunction in neurodegenerative diseases. Brain *142*, 2558-2571.

Braak, H., Del Tredici, K., Rub, U., de Vos, R.A., Jansen Steur, E.N., and Braak, E. (2003). Staging of brain pathology related to sporadic Parkinson's disease. NeurobiolAging *24*, 197-211.

Braak, H., Thal, D.R., Ghebremedhin, E., and Del Tredici, K. (2011). Stages of the pathologic process in Alzheimer disease: age categories from 1 to 100 years. Journal of neuropathology and experimental neurology *70*, 960-969.

Burbulla, L.F., Song, P., Mazzulli, J.R., Zampese, E., Wong, Y.C., Jeon, S., Santos, D.P., Blanz, J., Obermaier, C.D., Strojny, C., *et al.* (2017). Dopamine oxidation mediates mitochondrial and lysosomal dysfunction in Parkinson's disease. Science *357*, 1255-1261.

Cai, W., Wakamatsu, K., Zucca, F.A., Wang, Q., Yang, K., Mohamadzadehonarvar, N., Srivastava, P., Tanaka, H., Holly, G., Casella, L., *et al.* (2023). DOPA pheomelanin is increased in nigral neuromelanin of Parkinson's disease. Prog Neurobiol *223*, 102414.

Carballo-Carbajal, I., Laguna, A., Romero-Gimenez, J., Cuadros, T., Bove, J., Martinez-Vicente, M., Parent, A., Gonzalez-Sepulveda, M., Penuelas, N., Torra, A., *et al.* (2019). Brain tyrosinase overexpression implicates age-dependent neuromelanin production in Parkinson's disease pathogenesis. Nature communications *10*, 973.

Cebrian, C., Zucca, F.A., Mauri, P., Steinbeck, J.A., Studer, L., Scherzer, C.R., Kanter, E., Budhu, S., Mandelbaum, J., Vonsattel, J.P., *et al.* (2014). MHC-I expression renders catecholaminergic neurons susceptible to T-cell-mediated degeneration. NatCommun *5*, 3633.

Chand, D.A., Scadeng, M., and Dieriks, B.V. (2023). Absolute quantification of neuromelanin in formalin-fixed human brains using absorbance spectrophotometry. PloS one *18*, e0288327.

Chu, Y., and Kordower, J.H. (2007). Age-associated increases of alpha-synuclein in monkeys and humans are associated with nigrostriatal dopamine depletion: Is this the target for Parkinson's disease? NeurobiolDis *25*, 134-149.

Chuquilin-Arista, F., Alvarez-Avellon, T., and Menendez-Gonzalez, M. (2020). Prevalence of Depression and Anxiety in Parkinson Disease and Impact on Quality of Life: A Community-Based Study in Spain. Journal of geriatric psychiatry and neurology *33*, 207-213.

Cryan, J.F., Mombereau, C., and Vassout, A. (2005). The tail suspension test as a model for assessing antidepressant activity: review of pharmacological and genetic studies in mice. Neuroscience and biobehavioral reviews *29*, 571-625.

de Lau, L.M., and Breteler, M.M. (2006). Epidemiology of Parkinson's disease. Lancet Neurol *5*, 525-535.

Del Tredici, K., and Braak, H. (2013). Dysfunction of the locus coeruleus-norepinephrine system and related circuitry in Parkinson's disease-related dementia. J Neurol Neurosurg Psychiatry *84*, 774-783.

DelleDonne, A., Klos, K.J., Fujishiro, H., Ahmed, Z., Parisi, J.E., Josephs, K.A., Frigerio, R., Burnett, M., Wszolek, Z.K., Uitti, R.J., *et al.* (2008). Incidental Lewy body disease and preclinical Parkinson disease. ArchNeurol *65*, 1074-1080.

Fasano, M., Giraudo, S., Coha, S., Bergamasco, B., and Lopiano, L. (2003). Residual substantia nigra neuromelanin in Parkinson's disease is cross-linked to alpha-synuclein. NeurochemInt *42*, 603-606.

Fedorow, H., Halliday, G.M., Rickert, C.H., Gerlach, M., Riederer, P., and Double, K.L. (2006). Evidence for specific phases in the development of human neuromelanin. NeurobiolAging *27*, 506-512.

French, I.T., and Muthusamy, K.A. (2018). A Review of the Pedunculopontine Nucleus in Parkinson's Disease. Frontiers in aging neuroscience *10*, 99.

Gai, W.P., Geffen, L.B., Denoroy, L., and Blessing, W.W. (1993). Loss of C1 and C3 epinephrine-synthesizing neurons in the medulla oblongata in Parkinson's disease. Ann Neurol *33*, 357-367.

Giguere, N., Burke Nanni, S., and Trudeau, L.E. (2018). On Cell Loss and Selective Vulnerability of Neuronal Populations in Parkinson's Disease. Frontiers in neurology *9*, 455.

Gonzalez-Sepulveda, M., Compte, J., Cuadros, T., Nicolau, A., Guillard-Sirieix, C., Penuelas, N., Lorente-Picon, M., Parent, A., Romero-Gimenez, J., Cladera-Sastre, J.M., *et al.* (2023). In vivo reduction of age-dependent neuromelanin accumulation mitigates features of Parkinson's disease. Brain *146*, 1040-1052.

Gonzalez-Sepulveda, M., Laguna, A., Carballo-Carbajal, I., Galiano-Landeira, J., Romero-Gimenez, J., Cuadros, T., Parent, A., Penuelas, N., Compte, J., Nicolau, A., *et al.* (2020). Validation of a Reversed Phase UPLC-MS/MS Method to Determine Dopamine Metabolites and Oxidation Intermediates in Neuronal Differentiated SH-SY5Y Cells and Brain Tissue. ACS chemical neuroscience *11*, 2679-2687.

Grant, L.M., Richter, F., Miller, J.E., White, S.A., Fox, C.M., Zhu, C., Chesselet, M.F., and Ciucci, M.R. (2014). Vocalization deficits in mice over-expressing alpha-synuclein, a model of pre-manifest Parkinson's disease. Behavioral neuroscience *128*, 110-121.

Gratwicke, J., Kahan, J., Zrinzo, L., Hariz, M., Limousin, P., Foltynie, T., and Jahanshahi, M. (2013). The nucleus basalis of Meynert: a new target for deep brain stimulation in dementia? Neuroscience and biobehavioral reviews *37*, 2676-2688.

Greggio, E., Bergantino, E., Carter, D., Ahmad, R., Costin, G.E., Hearing, V.J., Clarimon, J., Singleton, A., Eerola, J., Hellstrom, O., *et al.* (2005). Tyrosinase exacerbates dopamine toxicity but is not genetically associated with Parkinson's disease. JNeurochem *93*, 246-256.

Halliday, G.M., Fedorow, H., Rickert, C.H., Gerlach, M., Riederer, P., and Double, K.L. (2006). Evidence for specific phases in the development of human neuromelanin. JNeural Transm *113*, 721-728.

Halliday, G.M., Li, Y.W., Blumbergs, P.C., Joh, T.H., Cotton, R.G., Howe, P.R., Blessing, W.W., and Geffen, L.B. (1990). Neuropathology of immunohistochemically identified brainstem neurons in Parkinson's disease. Ann Neurol *27*, 373-385.

Halliday, G.M., Ophof, A., Broe, M., Jensen, P.H., Kettle, E., Fedorow, H., Cartwright, M.I., Griffiths, F.M., Shepherd, C.E., and Double, K.L. (2005). Alpha-synuclein redistributes to neuromelanin lipid in the substantia nigra early in Parkinson's disease. Brain *128*, 2654-2664.

Herrero, M.T., Hirsch, E.C., Kastner, A., Luquin, M.R., Javoy-Agid, F., Gonzalo, L.M., Obeso, J.A., and Agid, Y. (1993). Neuromelanin accumulation with age in catecholaminergic neurons from Macaca fascicularis brainstem. Developmental neuroscience *15*, 37-48.

Hirsch, E., Graybiel, A.M., and Agid, Y.A. (1988). Melanized dopaminergic neurons are differentially susceptible to degeneration in Parkinson's disease. Nature *334*, 345-348.

Hirsch, E.C., and Hunot, S. (2009). Neuroinflammation in Parkinson's disease: a target for neuroprotection? Lancet Neurol *8*, 382-397.

Ikemoto, K., Nagatsu, I., Ito, S., King, R.A., Nishimura, A., and Nagatsu, T. (1998). Does tyrosinase exist in neuromelanin-pigmented neurons in the human substantia nigra? Neurosci Lett *253*, 198-200.

Ishikawa, A., and Takahashi, H. (1998). Clinical and neuropathological aspects of autosomal recessive juvenile parkinsonism. JNeurol *245*, 4-9.

Kemali, M., and Gioffre, D. (1985). Anatomical localisation of neuromelanin in the brains of the frog and tadpole. Ultrastructural comparison of neuromelanin with other melanins. Journal of anatomy *142*, 73-83.

Knudsen, K., Fedorova, T.D., Hansen, A.K., Sommerauer, M., Otto, M., Svendsen, K.B., Nahimi, A., Stokholm, M.G., Pavese, N., Beier, C.P., *et al.* (2018). In-vivo staging of pathology in REM sleep behaviour disorder: a multimodality imaging case-control study. Lancet Neurol *17*, 618-628.

Kordower, J.H., Olanow, C.W., Dodiya, H.B., Chu, Y., Beach, T.G., Adler, C.H., Halliday, G.M., and Bartus, R.T. (2013). Disease duration and the integrity of the nigrostriatal system in Parkinson's disease. Brain *136*, 2419-2431.

Korzhevskii, D.E., Kirik, O.V., Guselnikova, V.V., Tsyba, D.L., Fedorova, E.A., and Grigorev, I.P. (2021). Changes in cytoplasmic and extracellular neuromelanin in human substantia nigra with normal aging. European journal of histochemistry : EJH *65*.

Kuusisto, E., Parkkinen, L., and Alafuzoff, I. (2003). Morphogenesis of Lewy Bodies: Dissimilar Incorporation of a-Synuclein, Ubiquitin, and p62. JNeuropatholExpNeurol *62*, 1241-1253.

Langston, J.W., Forno, L.S., Tetrud, J., Reeves, A.G., Kaplan, J.A., and Karluk, D. (1999). Evidence of active nerve cell degeneration in the substantia nigra of humans years after 1-methyl-4-phenyl-1,2,3,6-tetrahydropyridine exposure. AnnNeurol *46*, 598-605.

Mann, D.M., and Yates, P.O. (1979). The effects of ageing on the pigmented nerve cells of the human locus caeruleous and substantia nigra. Acta Neuropathol *47*, 93-97.

Marsden, C.D. (1961). Pigmentation in the nucleus substantiae nigrae of mammals. JAnat *95*, 256-261.

McDevitt, R.A., Tiran-Cappello, A., Shen, H., Balderas, I., Britt, J.P., Marino, R.A.M., Chung, S.L., Richie, C.T., Harvey, B.K., and Bonci, A. (2014). Serotonergic versus nonserotonergic dorsal raphe projection neurons: differential participation in reward circuitry. Cell reports *8*, 1857-1869.

McRitchie, D.A., Cartwright, H.R., and Halliday, G.M. (1997). Specific A10 dopaminergic nuclei in the midbrain degenerate in Parkinson's disease. ExpNeurol *144*, 202-213.

Mena-Segovia, J., and Bolam, J.P. (2017). Rethinking the Pedunculopontine Nucleus: From Cellular Organization to Function. Neuron *94*, 7-18.

Miquel-Rio, L., Alarcon-Aris, D., Torres-Lopez, M., Coppola-Segovia, V., Pavia-Collado, R., Paz, V., Ruiz-Bronchal, E., Campa, L., Casal, C., Montefeltro, A., *et al.* (2022). Human alpha-synuclein overexpression in mouse serotonin neurons triggers a depressive-like phenotype. Rescue by oligonucleotide therapy. Translational psychiatry *12*, 79.

Miranda, M., Botti, D., Bonfigli, A., Ventura, T., and Arcadi, A. (1984). Tyrosinase-like activity in normal human substantia nigra. GenPharmacol *15*, 541-544.

Monzani, E., Nicolis, S., Dell'Acqua, S., Capucciati, A., Bacchella, C., Zucca, F., Mosharov, E., Sulzer, D., Zecca, L., and Casella, L. (2018). Dopamine, oxidative stress and protein-quinone modifications in Parkinson's and other neurodegenerative diseases. Angewandte Chemie.

Mor, D.E., Tsika, E., Mazzulli, J.R., Gould, N.S., Kim, H., Daniels, M.J., Doshi, S., Gupta, P., Grossman, J.L., Tan, V.X., *et al.* (2017). Dopamine induces soluble alpha-synuclein oligomers and nigrostriatal degeneration. Nature neuroscience *20*, 1560-1568.

Murer, M.G., Dziewczapolski, G., Menalled, L.B., Garcia, M.C., Agid, Y., Gershanik, O., and Raisman-Vozari, R. (1998). Chronic levodopa is not toxic for remaining dopamine neurons, but instead promotes their recovery, in rats with moderate nigrostriatal lesions. AnnNeurol *43*, 561-575.

Nagatsu, T., Nakashima, A., Ichinose, H., and Kobayashi, K. (2019). Human tyrosine hydroxylase in Parkinson's disease and in related disorders. Journal of neural transmission *126*, 397-409.

Plum, S., Steinbach, S., Attems, J., Keers, S., Riederer, P., Gerlach, M., May, C., and Marcus, K. (2016). Proteomic characterization of neuromelanin granules isolated from human substantia nigra by laser-microdissection. Scientific reports *6*, 37139.

Prettyman, R. (1998). Extrapyramidal signs in cognitively intact elderly people. Age Ageing *27*, 557-560.

Rajput, A.H., and Rozdilsky, B. (1976). Dysautonomia in Parkinsonism: a clinicopathological study. J Neurol Neurosurg Psychiatry *39*, 1092-1100.

Sacchini, S., Arbelo, M., Bombardi, C., Fernandez, A., Cozzi, B., Bernaldo de Quiros, Y., and Herraez, P. (2018). Locus coeruleus complex of the family Delphinidae. Scientific reports *8*, 5486.

Saper, C.B., and Petito, C.K. (1982). Correspondence of melanin-pigmented neurons in human brain with A1-A14 catecholamine cell groups. Brain *105*, 87-101.

Saper, C.B., Sorrentino, D.M., German, D.C., and de Lacalle, S. (1991). Medullary catecholaminergic neurons in the normal human brain and in Parkinson's disease. Ann Neurol *29*, 577-584.

Slominski, A., Tobin, D.J., Shibahara, S., and Wortsman, J. (2004). Melanin pigmentation in mammalian skin and its hormonal regulation. Physiol Rev *84*, 1155-1228.

Sulzer, D., Bogulavsky, J., Larsen, K.E., Behr, G., Karatekin, E., Kleinman, M.H., Turro, N., Krantz, D., Edwards, R.H., Greene, L.A., *et al.* (2000). Neuromelanin biosynthesis is driven by excess cytosolic catecholamines not accumulated by synaptic vesicles. ProcNatlAcadSciUSA *97*, 11869-11874.

Sulzer, D., and Surmeier, D.J. (2013). Neuronal vulnerability, pathogenesis, and Parkinson's disease. Mov Disord *28*, 715-724.

Szego, E.M., Gerhardt, E., Outeiro, T.F., and Kermer, P. (2011). Dopamine-depletion and increased alpha-synuclein load induce degeneration of cortical cholinergic fibers in mice. JNeurol Sci *310*, 90-95.

Tomlinson, B.E., Irving, D., and Blessed, G. (1981). Cell loss in the locus coeruleus in senile dementia of Alzheimer type. J Neurol Sci *49*, 419-428.

Tribl, F., Arzberger, T., Riederer, P., and Gerlach, M. (2007). Tyrosinase is not detected in human catecholaminergic neurons by immunohistochemistry and Western blot analysis. JNeural TransmSuppl, 51-55.

Tribl, F., Marcus, K., Meyer, H.E., Bringmann, G., Gerlach, M., and Riederer, P. (2006). Subcellular proteomics reveals neuromelanin granules to be a lysosome-related organelle. JNeural Transm *113*, 741-749.

Trulson, M.E., Cannon, M.S., and Raese, J.D. (1985). Identification of dopamine-containing cell bodies in the dorsal and median raphe nuclei of the rat brain using tyrosine hydroxylase immunochemistry. Brain research bulletin *15*, 229-234.

Tubert, C., Galtieri, D., and Surmeier, D.J. (2019). The pedunclopontine nucleus and Parkinson's disease. Neurobiology of disease *128*, 3-8.

Vila, M. (2019). Neuromelanin, aging, and neuronal vulnerability in Parkinson's disease. Movement disorders : official journal of the Movement Disorder Society.

Vila, M., Laguna, A., and Carballo-Carbajal, I. (2019). Intracellular crowding by age-dependent neuromelanin accumulation disrupts neuronal proteostasis and triggers Parkinson disease pathology. Autophagy *15*, 2028-2030.

Xing, Y., Sapuan, A., Dineen, R.A., and Auer, D.P. (2018). Life span pigmentation changes of the substantia nigra detected by neuromelanin-sensitive MRI. Movement disorders : official journal of the Movement Disorder Society *33*, 1792-1799.

Xu, Y., Stokes, A.H., Freeman, W.M., Kumer, S.C., Vogt, B.A., and Vrana, K.E. (1997). Tyrosinase mRNA is expressed in human substantia nigra. Brain ResMolBrain Res *45*, 159-162.

Zarow, C., Lyness, S.A., Mortimer, J.A., and Chui, H.C. (2003). Neuronal loss is greater in the locus coeruleus than nucleus basalis and substantia nigra in Alzheimer and Parkinson diseases. Archives of neurology *60*, 337-341.

Zecca, L., Stroppolo, A., Gatti, A., Tampellini, D., Toscani, M., Gallorini, M., Giaveri, G., Arosio, P., Santambrogio, P., Fariello, R.G., *et al.* (2004). The role of iron and copper molecules in the neuronal vulnerability of locus coeruleus and substantia nigra during aging. Proc Natl Acad Sci U S A *101*, 9843-9848.

Zucca, F.A., Basso, E., Cupaioli, F.A., Ferrari, E., Sulzer, D., Casella, L., and Zecca, L. (2014). Neuromelanin of the human substantia nigra: an update. Neurotox Res *25*, 13-23.

Zucca, F.A., Capucciati, A., Bellei, C., Sarna, M., Sarna, T., Monzani, E., Casella, L., and Zecca, L. (2023). Neuromelanins in brain aging and Parkinson's disease: synthesis, structure, neuroinflammatory, and neurodegenerative role. IUBMB life *75*, 55-65.

Zucca, F.A., Vanna, R., Cupaioli, F.A., Bellei, C., De Palma, A., Di Silvestre, D., Mauri, P., Grassi, S., Prinetti, A., Casella, L., *et al.* (2018). Neuromelanin organelles are specialized autolysosomes that accumulate undegraded proteins and lipids in aging human brain and are likely involved in Parkinson's disease. NPJ Parkinson's disease *4*, 17.

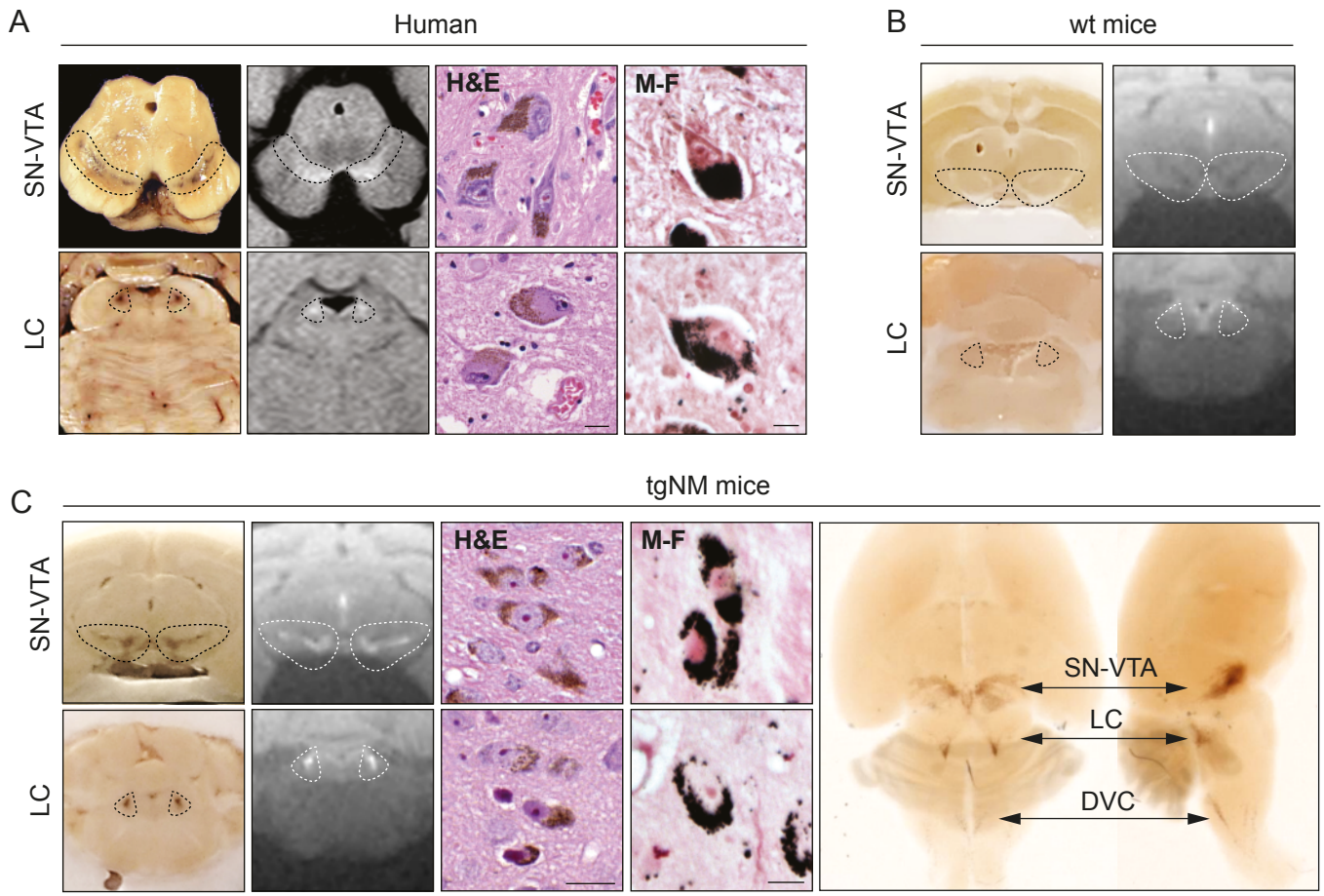
A
Human
SN-VTA
LC
H&E
M-F
B
wt mice
SN-VTA
LC
C
tgNM mice
SN-VTA
LC
H&E
M-F
SN-VTA
LC
DVC

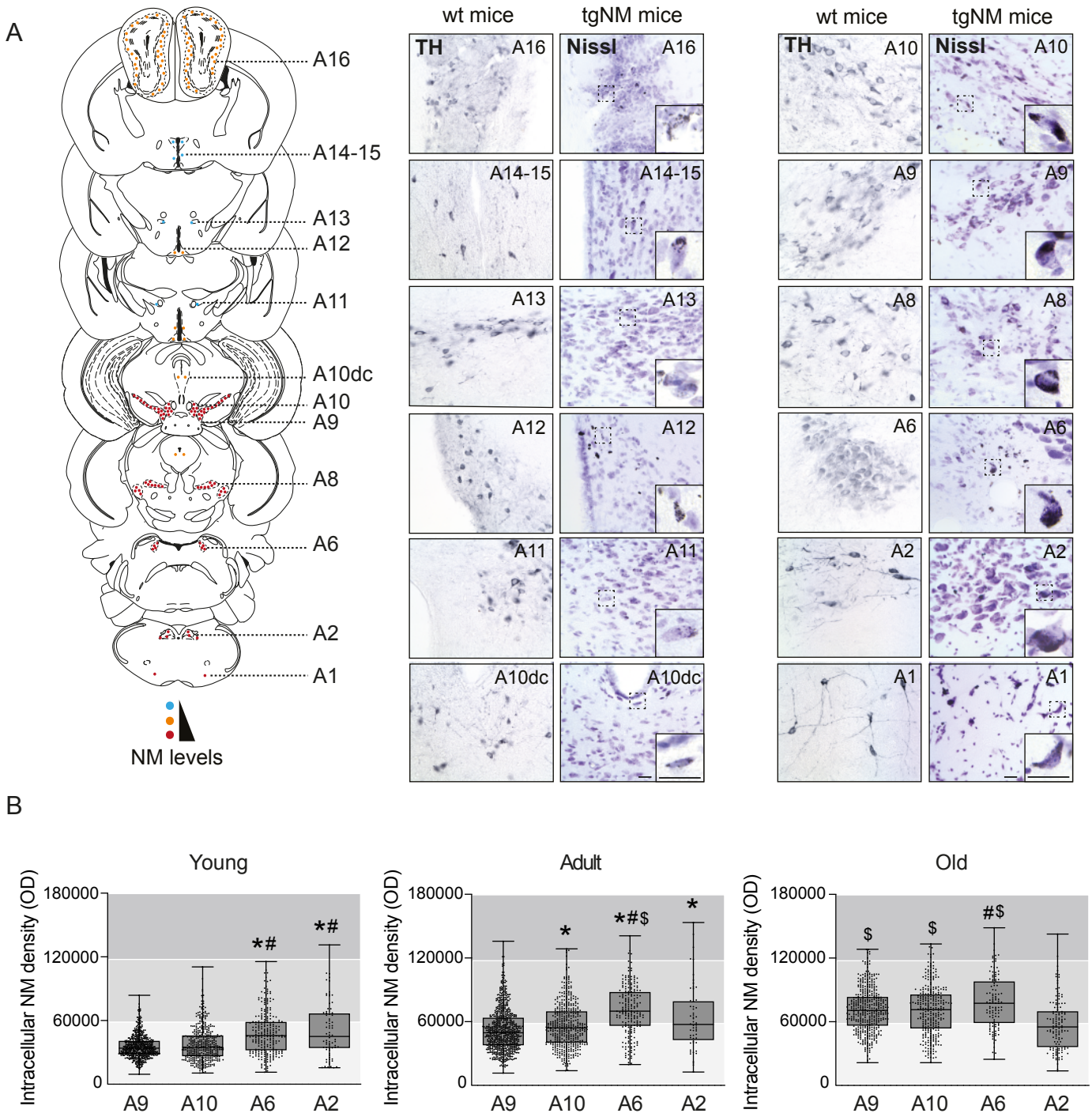
A
A16
A14-15
A13
A12
A11
A10dc
A10
A9
A8
A6
A2
A1
NM levels
wt mice
tgNM mice
TH
Nissl
B
Young
Adult
Old
Intracellular NM density (OD)
180000
120000
60000
0
A9
A10
A6
A2
*#
*#$
*
$
#$

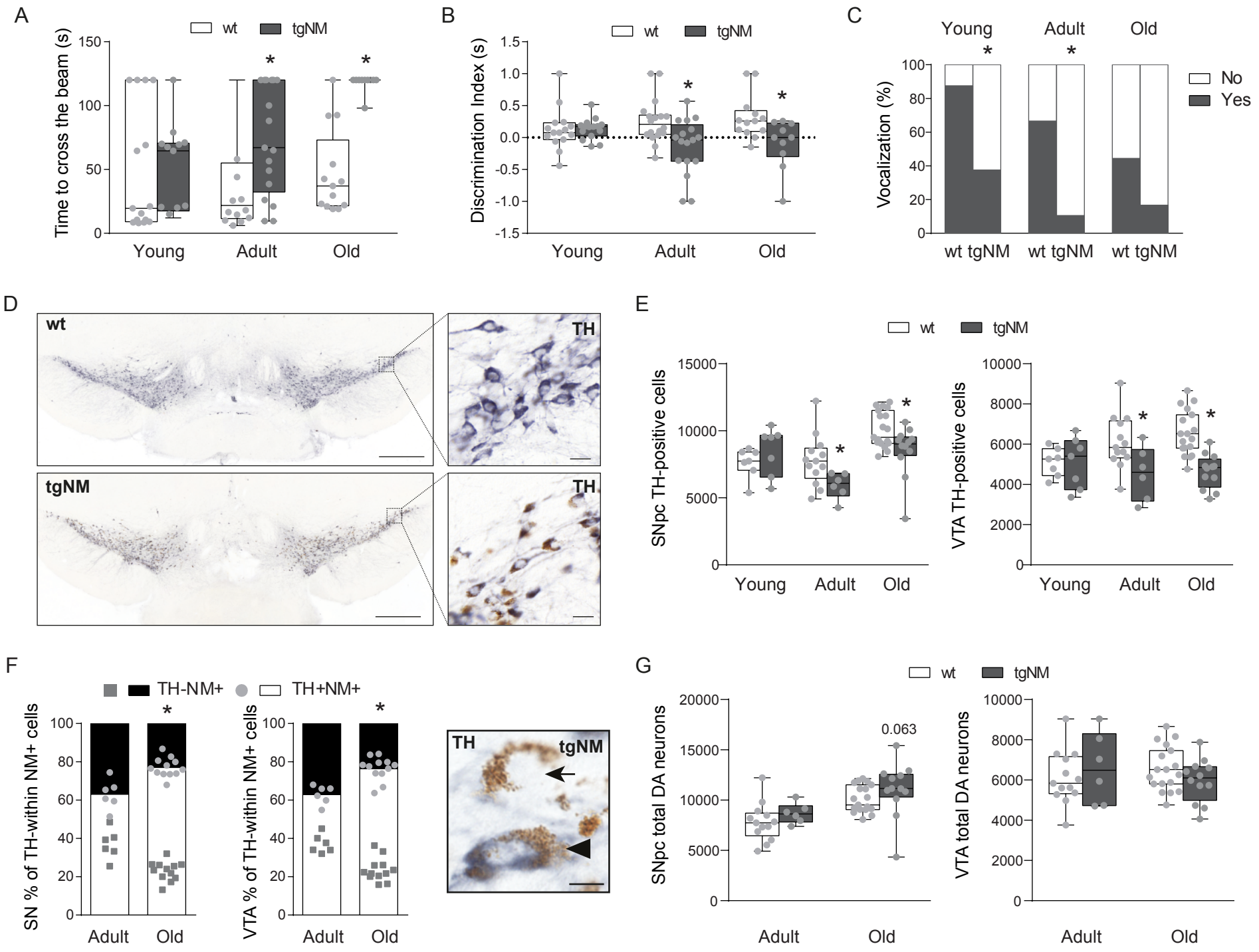
A
wt
tgNM
Time to cross the beam (s)
150
100
50
0
*
*
Young
Adult
Old
B
wt
tgNM
Discrimination Index (s)
1.5
1.0
0.5
0.0
-0.5
-1.0
-1.5
*
*
Young
Adult
Old
C
Young
Adult
Old
Vocalization (%)
100
80
60
40
20
0
*
*
No
Yes
wt tgNM
wt tgNM
wt tgNM
D
wt
TH
tgNM
TH
E
wt
tgNM
SNpc TH-positive cells
15000
10000
5000
0
*
*
Young
Adult
Old
VTA TH-positive cells
10000
8000
6000
4000
2000
0
*
*
Young
Adult
Old
F
TH-NM+
TH+NM+
SN % of TH-within NM+ cells
100
80
60
40
20
0
*
Adult
Old
VTA % of TH-within NM+ cells
100
80
60
40
20
0
*
Adult
Old
TH
tgNM
G
wt
tgNM
SNpc total DA neurons
20000
15000
10000
5000
0
0.063
Adult
Old
VTA total DA neurons
10000
8000
6000
4000
2000
0
Adult
Old

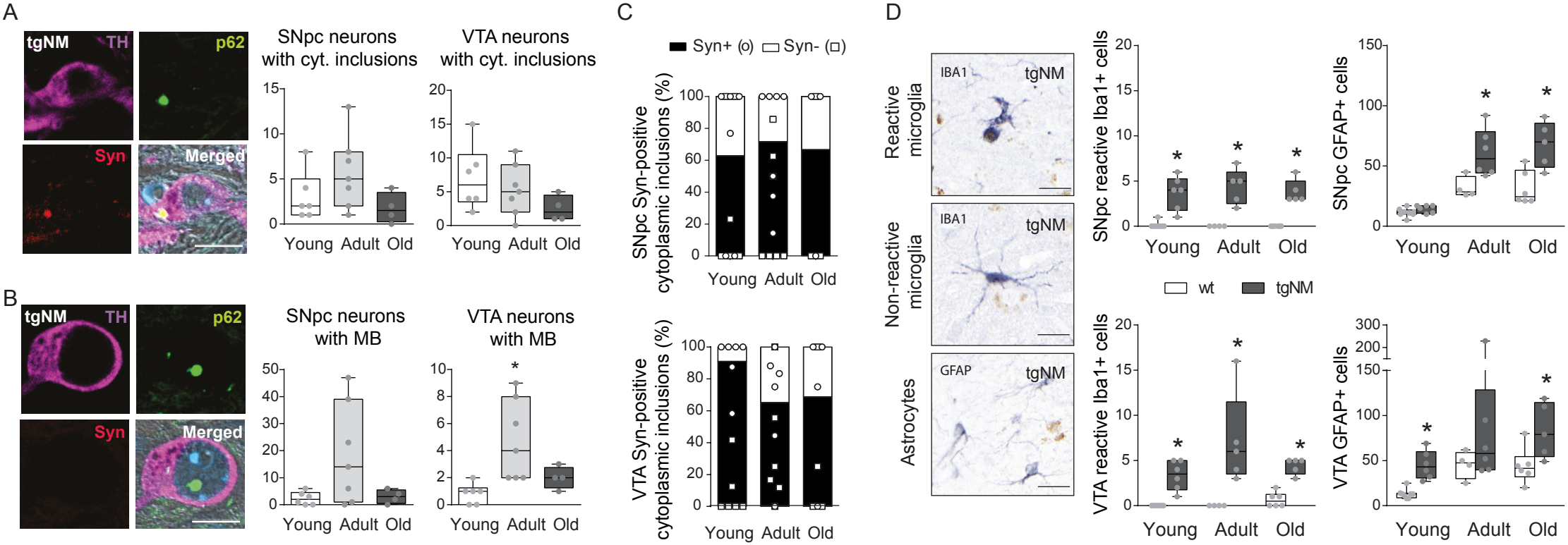
A
tgNM
TH
p62
Syn
Merged
SNpc neurons with cyt. inclusions
VTA neurons with cyt. inclusions
Young Adult Old
B
SNpc neurons with MB
VTA neurons with MB
C
Syn+ (o) Syn- (□)
SNpc Syn-positive cytoplasmic inclusions (%)
VTA Syn-positive cytoplasmic inclusions (%)
D
Reactive microglia
Non-reactive microglia
Astrocytes
IBA1
GFAP
SNpc reactive Iba1+ cells
SNpc GFAP+ cells
VTA reactive Iba1+ cells
VTA GFAP+ cells
wt
tgNM

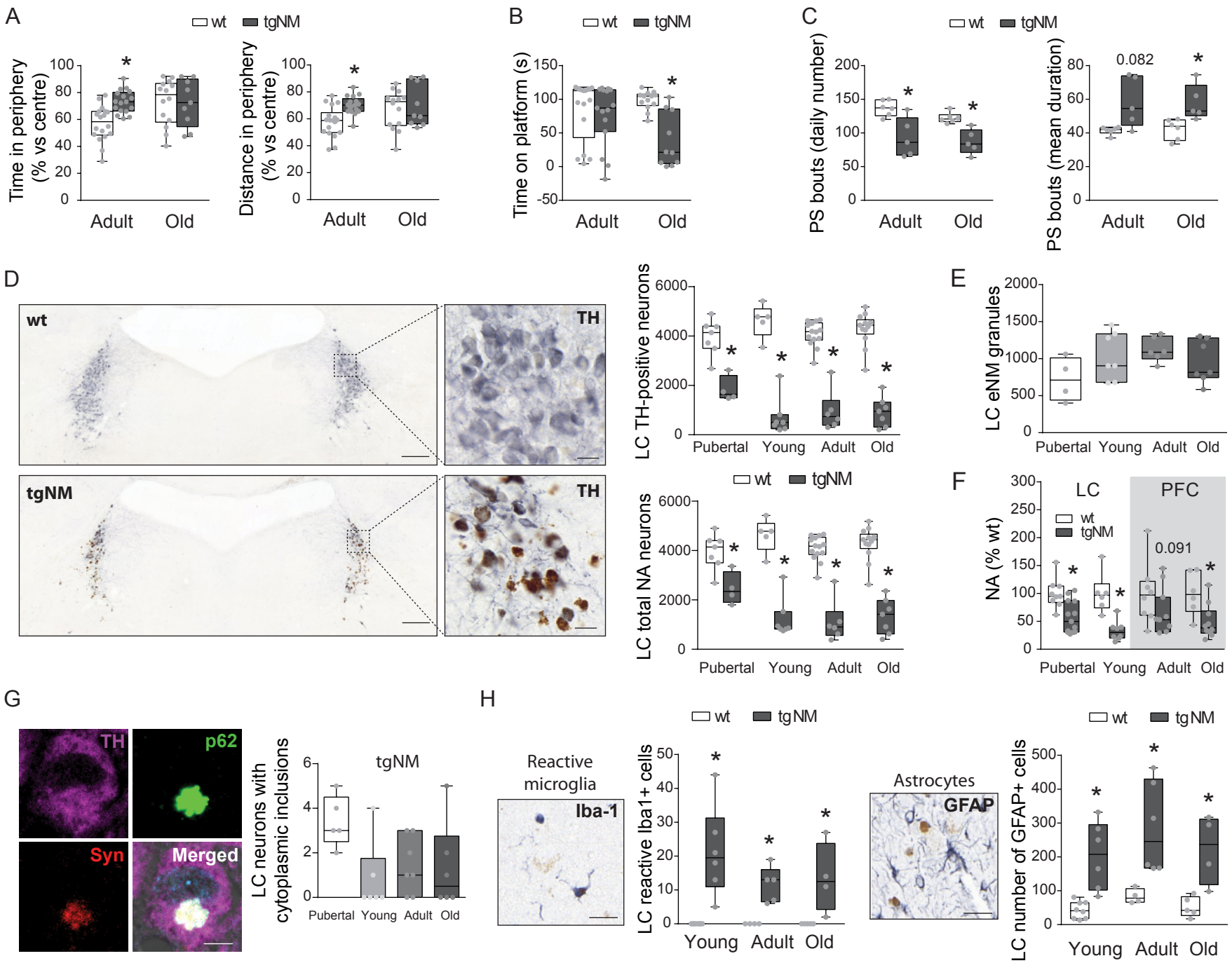
A
wt
tgNM
Time in periphery (% vs centre)
Distance in periphery (% vs centre)
Adult
Old
B
Time on platform (s)
C
PS bouts (daily number)
PS bouts (mean duration)
0.082
D
wt
tgNM
TH
LC TH-positive neurons
LC total NA neurons
Pubertal
Young
E
LC eNM granules
F
LC
PFC
NA (% wt)
0.091
G
TH
p62
Syn
Merged
LC neurons with cytoplasmic inclusions
H
Reactive microglia
Iba-1
LC reactive Iba1+ cells
Astrocytes
GFAP
LC number of GFAP+ cells

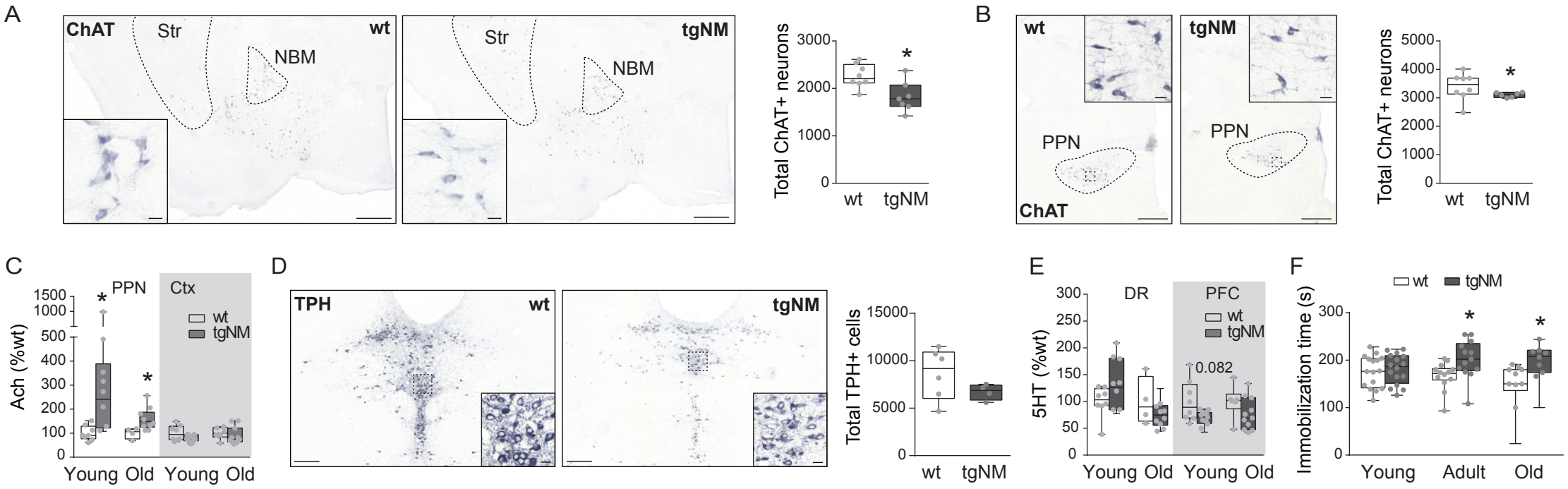
A
ChAT
Str
NBM
wt
tgNM
Total ChAT+ neurons
3000
2000
1000
0
wt
tgNM
*
B
wt
tgNM
PPN
ChAT
Total ChAT+ neurons
5000
4000
3000
2000
1000
0
C
PPN
Ctx
wt
tgNM
Ach (%wt)
1500
1000
500
400
300
200
100
0
Young Old Young Old
D
TPH
Total TPH+ cells
15000
10000
5000
E
DR
PFC
5HT (%wt)
300
250
200
150
100
50
0.082
F
Immobilization time (s)
Young
Adult
Old

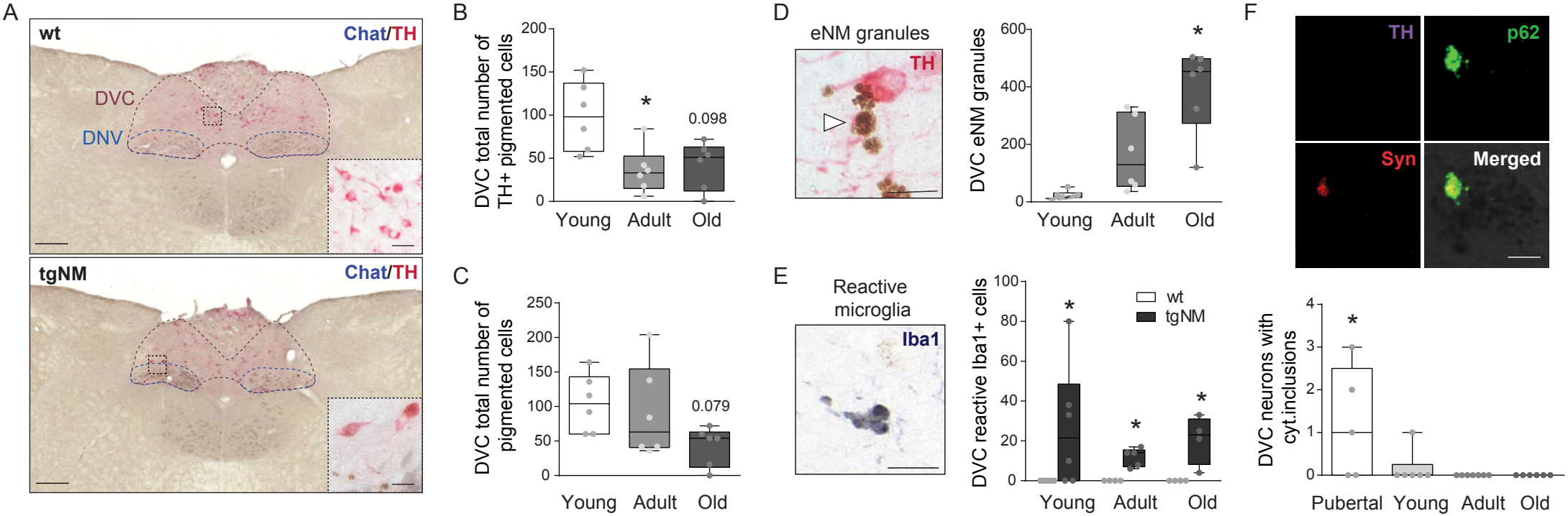
A
wt
Chat/TH
DVC
DNV
tgNM
Chat/TH
B
DVC total number of TH+ pigmented cells
200
150
100
50
0
*
0.098
Young
Adult
Old
C
DVC total number of pigmented cells
250
200
150
100
50
0
0.079
Young
Adult
Old
D
eNM granules
TH
DVC eNM granules
600
400
200
0
*
Young
Adult
Old
E
Reactive microglia
Iba1
DVC reactive Iba1+ cells
100
80
60
40
20
0
wt
tgNM
*
*
*
Young
Adult
Old
F
TH
p62
Syn
Merged
DVC neurons with cyt.inclusions
4
3
2
1
0
*
Pubertal
Young
Adult
Old

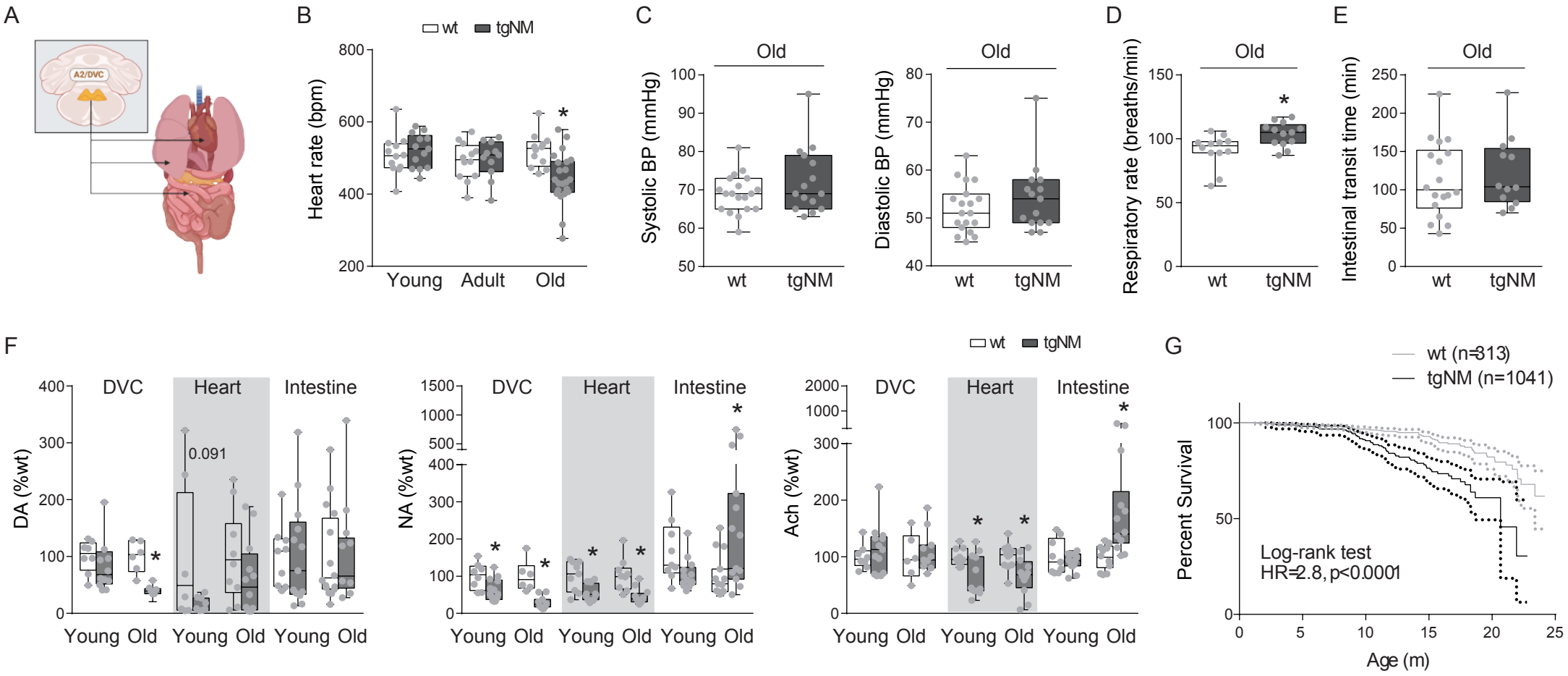
A
A2/DVC
B
wt
tgNM
Heart rate (bpm)
800
600
400
200
Young
Adult
Old
*
C
Old
Systolic BP (mmHg)
100
90
80
70
60
50
wt
tgNM
Old
Diastolic BP (mmHg)
80
70
60
50
40
wt
tgNM
D
Old
Respiratory rate (breaths/min)
150
100
50
0
*
wt
tgNM
E
Old
Intestinal transit time (min)
250
200
150
100
50
0
wt
tgNM
F
DVC
Heart
Intestine
DA (%wt)
400
300
200
100
0
0.091
*
Young Old Young Old Young Old
NA (%wt)
1500
1000
500
400
300
200
100
0
*
Young Old Young Old Young Old
wt
tgNM
Ach (%wt)
2000
1000
300
200
100
0
*
Young Old Young Old Young Old
G
wt (n=313)
tgNM (n=1041)
Percent Survival
100
50
0
Log-rank test
HR=2.8, p<0.0001
0
5
10
15
20
25
Age (m)